Electrosorption Valency and Partial Charge Transfer in Halide and Sulfide Adsorption on Ag(111)

ARTICLE *in* LANGMUIR · NOVEMBER 1998

Impact Factor: 4.46 · DOI: 10.1021/la980692t

4 AUTHORS, INCLUDING:

Maria Luisa Foresti
University of Florence
115 PUBLICATIONS **1,929** CITATIONS
SEE PROFILE

Rolando Guidelli
University of Florence
226 PUBLICATIONS **3,838** CITATIONS
SEE PROFILE

Electrosorption Valency and Partial Charge Transfer in Halide and Sulfide Adsorption on Ag(111)

Maria Luisa Foresti, Massimo Innocenti, Francesca Forni, and Rolando Guidelli*

Dipartimento di Chimica, Universita' di Firenze, Via G. Capponi 9, 50121 Firenze, Italy

Received June 15, 1998. In Final Form: September 7, 1998

The electrosorption valency l_B of an adsorbed species is usually obtained from the slope of plots of the charge density on the metal against the surface concentration of the given species, at constant applied potential. Herein, two alternative procedures for the estimate of l_B are proposed and applied to the formation of ordered overlayers of chloride, bromide, iodide, and sulfide on Ag(111). One of these procedures applies to strongly adsorbing anions, whose incipient adsorption turns out to be diffusion controlled under limiting conditions when stepping from a potential negative enough to exclude their specific adsorption. This procedure allows l_B to be estimated as a function of the applied potential. Partial charge-transfer coefficients λ estimated from l_B values on the basis of some modelistic assumptions decrease in the order sulfide ≈ iodide > bromide > chloride, namely in the order of increasing Pauling's electronegativity. Some direct procedures for the estimate of λ, which avoid the intermediate estimate of l_B, are shown to lead to erroneous results.

Introduction

In the chemisorption of a substance A^z on a metal electrode from an electrolytic solution, the substance comes in direct contact with the electrode surface. Depending on the nature of the substance and of the electrode material, chemisorption may be accompanied by partial charge transfer (pct) from the adsorbate to the metal substrate:

$$A^z(\text{solution}) \Leftrightarrow A^{z+\lambda}(\text{adsorbed}) + \lambda e^-$$

The quantity λ is called the partial charge-transfer coefficient. Lorentz and Salie,[1] as well as Vetter and Schultze et al.,[2] considered the concept of partial charge transfer from somewhat different viewpoints. In particular, Vetter and Schultze[2a] proposed to estimate the extent of pct on the basis of the thermodynamic quantity called "electrosorption valency" l_B. For an ionic species of charge number z, the electrosorption valency is defined as

$$l_B = -z\left(\frac{\partial\sigma_M}{\partial\sigma_i}\right)_E \qquad (1)$$

where σ_M and σ_i are the charge density on the metal and that due to the specifically adsorbed species and E is the applied potential. This equation holds strictly in the presence of an excess of a nonspecifically adsorbed electrolyte; otherwise, E is to be replaced by the potential difference across the inner layer. The rationale behind this definition is the following: if the chemisorption of the ion at constant applied potential is accompanied by a flow of an amount of electrons of equal and opposite charge along the external circuit, then the electrosorption valency coincides with the charge number z of the ion. This situation is encountered only under particular conditions.

Imagine adding a specifically adsorbed anion to a solution containing a strong excess of a nonspecifically adsorbed electrolyte and imagine following its adsorption at the metal/water interface, at constant applied potential. If, ab absurdo, the anion were itself nonspecifically adsorbed, and hence had not to be deprived of its solvation sheath on the metal side in its position of closest approach to the electrode surface, then it would be accompanied in this approach by a nonspecifically adsorbed cation, and hence no flow of electrons along the external circuit would be observed. This situation is depicted schematically in Figure 1a, where x is the distance from the electrode surface and $x = d$ is the distance of closest approach of the nonspecifically adsorbed ions to the electrode. The potential−distance profile is represented schematically by curve 1. Since, however, the anion is specifically adsorbed, it will actually be deprived of its solvation sheath on the metal side, bringing its center of charge to the distance $x = \beta$ from the electrode surface, which is shorter than $x = d$, as shown in Figure 1b. This gives rise to a negative potential drop between the $x = \beta$ and $x = d$ planes, represented by curve 2 in Figure 1b. For a constant potential difference $\Delta\phi$ across the inner layer, this negative contribution to $\Delta\phi$ must be compensated for by a positive contribution, which is produced by a positive shift $\Delta\sigma_M$ in the charge density on the metal from $\sigma_M°$ to σ_M. The contribution from the new charge density σ_M to the potential drop between $x = 0$ and $x = d$ is represented schematically by curve 3 in Figure 1b, while the overall potential-distance profile is represented by curve 1. If the anion also transfers a fraction λ of its negative charge to the electrode upon chemisorption, the positive shift $\Delta\sigma_M$ will be greater. Unfortunately, the estimate of λ from the electrosorption valency l_B requires a number of modelistic assumptions. Thus, for instance, screening of the charge of the adsorbed ion by the inhomogeneous electron gas and by the solvent molecules produces an effect analogous to that of partial charge transfer.[3,4] Nonetheless, if the

(1) (a) Lorenz, W.; Salie, G. *Z. Phys. Chem. (Leipzig)* **1961**, *218*, 259. (b) Lorenz, W.; Salie, G. *J. Electroanal. Chem.* **1977**, *80*, 1.

(2) (a) Vetter, K. J.; Schultze, J. W. *Ber. Bunsen-Ges. Phys. Chem.* **1972**, *76*, 6, 920, 927. (b) Schultze, J. W.; Vetter, K. J. *J. Electroanal. Chem.* **1973**, *44*, 63. (c) Schultze, J. W.; Koppitz, F. D. *Electrochim. Acta* **1976**, *21*, 327. (d) Koppitz, F. D.; Schultze, J. W. *Electrochim. Acta* **1976**, *21*, 337. (e) Koppitz, F. D.; Schultze, J. W.; Rolle, D. *J. Electroanal. Chem.* **1984**, *170*, 5. (f) Rolle, D.; Schultze, J. W. *Electrochim. Acta* **1986**, *31*, 991. (g) Rolle, D.; Schultze, J. W. *J. Electroanal. Chem.* **1987**, *229*, 141.

(3) Lang, N. D.; Williams, A. R. *Phys. Rev. B* **1978**, *18*, 616.

10.1021/la980692t CCC: $15.00
Published on Web 11/06/1998

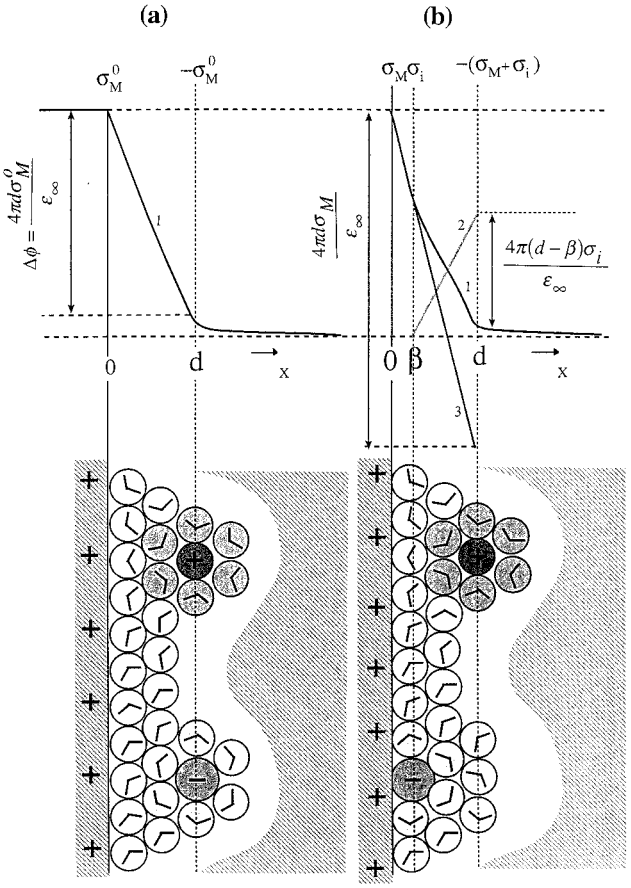

Figure 1. Schematic picture of the metal/solution interphase in the case of nonspecific (a) and specific (b) anionic adsorption. $x = 0$, $x = \beta$, and $x = d$ are the electrode surface plane, the plane of closest approach for the specifically adsorbed anions, and that for the nonspecifically adsorbed ions. Curve 1 represents the potential−distance profile. In part b, curve 1 results from the combination of curve 2, expressing the contribution from the charge density σ_i of the specifically adsorbed anions, and curve 3, expressing the contribution from the charge density σ_M on the metal. The potential difference $\Delta\phi$ across the inner layer is the same in parts a and b.

l_B values for a series of compounds of similar structure show a definite trend, this may provide useful information on the corresponding trend of their partial charge-transfer coefficients.

The electrosorption valency is normally estimated from the slope of plots of σ_M against the surface concentration Γ_i of the adsorbing species at constant E, or else (which is thermodynamically equivalent) from the slope of plots of the Gibbs energy of adsorption against the applied potential at constant Γ_i.[2a−c] Since the extent of pct may depend on surface coverage, l_B is conveniently estimated by measuring the limiting value of the slope of the σ_M versus Γ_i plots for $\Gamma_i \rightarrow 0$. In the case of highly surface active anions, such an extrapolation may be inaccurate, especially at the more positive potentials: here adsorption is so strong that the attainment of low surface coverages is practically impossible, since it would require prohibitively low bulk concentrations. This article describes two alternative procedures for the estimate of the electrosorption valency, which do not suffer from this limitation. These procedures are applied to the chemisorption of sulfide and halide ions on Ag(111) from aqueous solutions. The correlation between the resulting l_B values and Pauling's electronegativity χ indicates that λ decreases progressively with increasing χ.

Experimental Section

Merck Suprapur KI, KBr, and KCl were baked at 400 °C to remove organic impurities. Merck Suprapur NaOH and Aldrich analytical reagent grade Na_2S were used without further purification. Jansen analytical reagent grade KPF_6 was purified as described in refs 5 and 6. The water used was obtained from light mineral water by distilling it once and by then distilling the water so obtained from alkaline permanganate while discarding the heads. The working electrodes were cylindrical silver crystals grown in a graphite crucible, oriented by X-rays, and cut according to the Bridgman technique.[7] These electrodes were polished with successively finer grades of alumina power down to 0.3 μm (Buehler Micropolish II) and then annealed in a muffle furnace under vacuum for 30 min at 650 °C. Before each electrochemical measurement the electrode was polished chemically with CrO_3 according to the procedure described in ref 8. After polishing, the electrode surface was soaked in concentrated sulfuric acid for about 20 min and then rinsed thoroughly with water.

A gold wire was used as a counter electrode, and an external saturated calomel electrode (SCE) served as reference; all potentials are referred to this electrode. The four-electrode potentiostatic system by Herrmann et al.[9] was employed to minimize the noise, and positive feedback circuitry was utilized to correct for the uncompensated resistance. The hanging solution method[10] was employed. The cell was water-jacketed and thermostated at 25 ± 0.2 °C. The solution was deaerated with argon, that was bubbled into the solution before measurements and blown over the solution during them. The cylindrical single-crystal electrode was held by a silver wire sealed into a glass tube which was secured to a movable stand. The stand was connected to a digital position sensor, which permitted us to estimate a 0.1 mm vertical shift of the stand. Cyclic voltammetric and chronocoulometric measurements were carried out under the control of a Data General DG10 microcomputer: the voltage signal, modulated according to the technique employed, was generated by the microcomputer through digital-to-analog conversion and applied to the cell via an Amel Model 551 fast-rise potentiostat.

Sulfide and iodide adsorption was investigated in the presence of 0.15 M NaOH. This excess of NaOH allowed the onset of hydrogen evolution to be shifted to potentials negative of those at which sulfide and iodide are no longer specifically adsorbed. Bromide adsorption was investigated in the presence of an excess (0.1 M) of KPF_6. Chloride adsorption was investigated from mixed cM KCl + (0.1 − c) M KPF_6 solutions.

The charge density σ_M on the metal as a function of the applied potential E was estimated by potential-step chronocoulometry. The detailed experimental procedure is described in ref 11. Briefly, the applied potential was stepped from a variable initial value E to a fixed final value E_f negative enough to exclude specific adsorption of the anions under study. The rest of the time of the electrode at E was made long enough to ensure attainment of adsorption equilibrium. The initial potential E was varied progressively by 25 mV increments, and the current following each potential jump $E \rightarrow E_f$ was integrated over time. The resulting charge versus potential curves were converted into σ_M versus E curves by forcing them to coincide at E_f and by then setting the common σ_M value at E_f equal to that for 0.1 M KPF_6 in the case of bromide and chloride and to that for 0.15 M KPF_6

(4) (a) Schmickler, W.; Guidelli, R. *J. Electroanal. Chem.* **1987**, *235*, 387. (b) Schmickler, W. *J. Electroanal. Chem.* **1988**, *249*, 25.

(5) Fawcett, W. R.; Mackey, M. D. *J. Chem. Soc., Faraday Trans. 1* **1973**, *69*, 634.

(6) Hills, G. S.; Reeves, R. H. *J. Electroanal. Chem.* **1971**, *31*, 269.

(7) Hamelin, A. In *Modern Aspects of Electrochemistry*; Conway, B. E., White, R. E., Bockris, J. O'M., Eds.; Plenum Press: New York, 1985; Vol. 16, p 1.

(8) Hamelin, A.; Stoicoviciu, L.; Doubova, L.; Trasatti, S. *J. Electroanal. Chem.* **1988**, *244*, 133.

(9) Herrmann, C. C.; Perrault, G. G.; Konrad, D.; Pilla, A. A. *Bull. Soc. Chim. Fr.* **1972**, *12*, 4468.

(10) Dickertmann, D.; Schultze, J. W.; Koppitz, F. D. *Electrochim. Acta* **1976**, *21*, 967.

(11) Foresti, M. L.; Innocenti M.; Hamelin, A. *Langmuir* **1995**, *11*, 498.

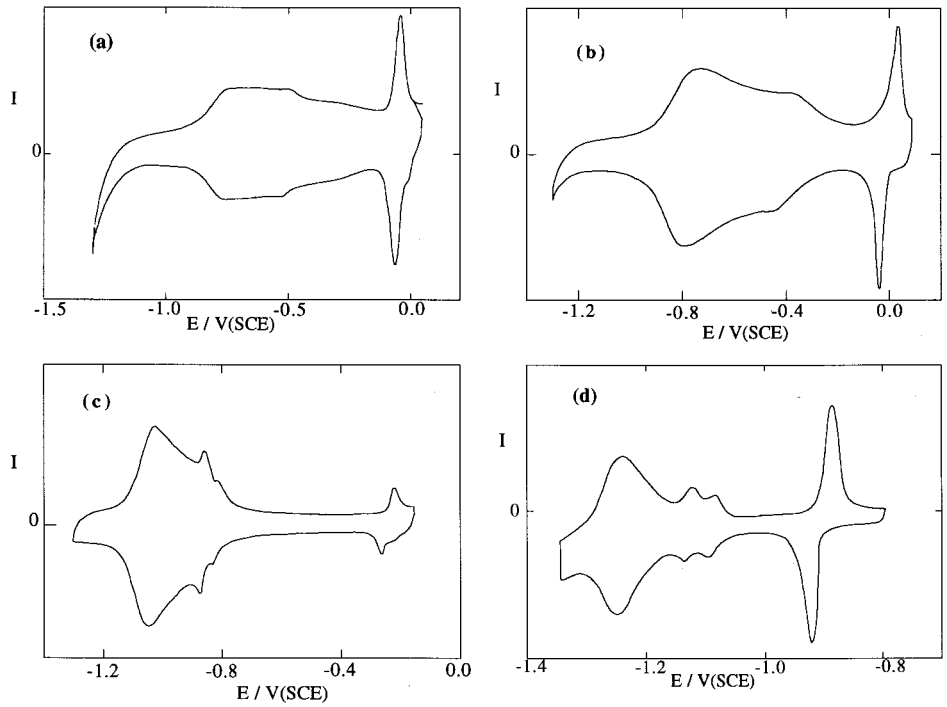

Figure 2. Cyclic voltammograms on Ag(111) from solutions of 5×10^{-4} M KCl + 0.1 M KPF_6 (a), 5×10^{-4} M KBr + 0.1 M KPF_6 (b), 5×10^{-4} M KI + 0.15 M NaOH (c), and 5×10^{-4} M Na_2S + 0.15 M NaOH (d).

in the case of sulfide and iodide. The potential of zero charge for the nonspecifically adsorbed KPF_6 was estimated from the minimum in the corresponding curve of the differential capacity against E.

Results

Figure 2 shows the cyclic voltammograms of Cl^-, Br^-, I^-, and S^{2-} ions on Ag(111) from aqueous solutions containing an excess of a different electrolyte. At the most positive potentials, all cyclic voltammograms in Figure 2 show a sharp peak, which is preceded by a relatively flat minimum. Over the potential region of the minimum, in situ STM images reveal a $(\sqrt{3}\times\sqrt{3})$R30° structure for all anions[12,13] but chloride ion. With the latter ion, no atomic resolution was obtained along the flat minimum; only occasionally were small islands with a $(\sqrt{3}\times\sqrt{3})$R30° structure observed. The sharp peak marks the transition to a more compressed overlayer structure, as revealed by in situ STM. Thus, at potentials positive of the peak, sulfide adsorption is characterized by a $(\sqrt{7}\times\sqrt{7})$R19.1° structure, where each lattice site is occupied by a triplet of sulfur atoms.[13] Bromide chemisorption at potentials positive of the sharp peak also yields a $(\sqrt{7}\times\sqrt{7})$R19.1° structure.[12] This structure is characterized by a unit cell with two atoms inside and four at the four vertexes; along any given row the atoms are adsorbed over a succession of two 3-fold hollow sites and one top site. Both $(\sqrt{7}\times\sqrt{7})$-R19.1° structures yield a $^3/_7$ fractional coverage. Because of their larger size, iodide ions give rise to a slightly less compressed structure at potentials positive of the sharp peak; it consists of a corrugated (8×8)R0° structure, where along any given row every eighth iodide ion is aligned with the underlying silver atom and constitutes the top of the corresponding corrugation.[12] Finally, the ordered overlayer of chloride ions at potentials positive of the sharp peak is characterized by a (1.38×1.38)R0° structure.[14,15] Table 1 summarizes the structures of the various anions before and after the sharp peak, and the corresponding surface concentrations Γ_i, calculated for an ideal Ag(111) face. Γ_i values can also be obtained by a thermodynamical analysis of σ_M versus E curves. Here we are interested in the limiting surface concentrations corresponding to the ordered overlayer structures. Hence, only bulk anionic concentrations high enough to reach these limiting Γ_i values over a sufficiently wide potential range were employed. Figure 3 shows σ_M versus E curves of halide and sulfide ions at bulk concentrations satisfying the above requirements. For comparison, this figure also shows curves of the charge density $\sigma_M°$ of the nonspecifically adsorbed KPF_6 electrolyte[16] against E; the KPF_6 concentration in these curves is equal to the overall salt concentration in the corresponding σ_M versus E curves. Therefore, over the potential range of stability of the ordered overlayers, the vertical distance between the σ_M versus E curves and the corresponding $\sigma_M°$ versus E curves provides the difference between the charge density in the presence of the overlayer and that in the absence of specific adsorption, at the same applied potential and ionic strength. In fact, even when using 0.15 M NaOH as supporting electrolyte in order to shift hydrogen discharge to more negative potentials, the formation of an ordered overlayer of sulfide or iodide ions prevents the chemisorption of NaOH. All σ_M versus E curves show two steps, with two distinct plateaus that run approximately parallel to the $\sigma_M°$ versus E curves. The first plateau corresponds to the $(\sqrt{3}\times\sqrt{3})$R30° structure, with the only exception being for chloride ion; the second plateau corresponds to the more compressed overlayer. An increase in the anionic bulk concentration merely causes a gradual shift of the two steps toward more negative

(12) Foresti, M. L.; Aloisi, G.; Innocenti, M.; Kobayashi, H.; Guidelli, R. *Surf. Sci.* **1995**, *335*, 241.
(13) Aloisi, G. D.; Cavallini, M.; Innocenti, M.; Foresti, M. L.; Pezzatini, G.; Guidelli, R. *J. Phys. Chem.* **1997**, *101*, 4774.
(14) Zei, M. S. *J. Electroanal. Chem.* **1991**, *308*, 295.
(15) Aloisi, G.; Funtikov, A. M.; Will, T. *J. Electroanal. Chem.* **1994**, *370*, 297.
(16) Valette, G. *J. Electroanal. Chem.* **1981**, *122*, 285.

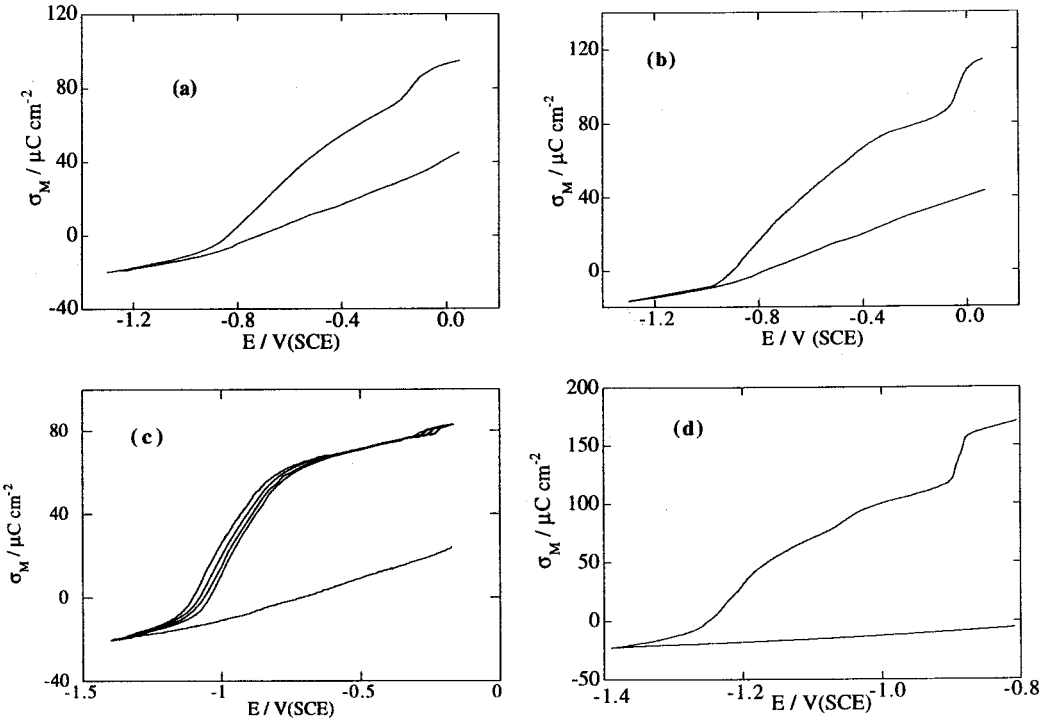

Figure 3. Upper curves are σ_M versus E plots on Ag(111) obtained from solutions of 5×10^{-2} M KCl + 5×10^{-2} M KPF_6 (a), 5×10^{-4} M KBr + 0.1 M KPF_6 (b), KI + 0.15 M NaOH (c), and 1×10^{-3} M Na_2S + 0.15 M NaOH (d), by jumping from a variable initial potential E to a fixed final potential equal to −1.30 V (a), −1.30 V (b), −1.40 V (c), and −1.40 V (d). In part c, the KI concentration equals 9.2×10^{-5}, 1.66×10^{-4}, 3×10^{-4}, and 5×10^{-4} M, when proceeding from right to left. The lower curves are plots of the charge density $\sigma_M°$ of KPF_6 solutions of concentration equal to the overall salt concentration of the corresponding upper curves.

Table 1.

anion	overlayer structure	$10^{10}\,\Gamma_i$ (mol cm^{-2}) structural	$10^{10}\,\Gamma_i$ (mol cm^{-2}) thermodynamic	$l_{B,int}/z$	λ	Pauling electronegativity χ
S^{2-}	$(\sqrt{3}\times\sqrt{3})$R30°	7.67	7.98	0.85	1.51	2.5
	$(\sqrt{7}\times\sqrt{7})$R19.1°	9.86		0.98	1.94	
I^-	$(\sqrt{3}\times\sqrt{3})$R30°	7.67	8.30	0.86	0.81	2.5
	(8×8)R0°	9.69				
Br^-	$(\sqrt{3}\times\sqrt{3})$R30°	7.67	8.50	0.65	0.46	2.8
	$(\sqrt{7}\times\sqrt{7})$R19.1°	9.86		0.77	0.65	
Cl^-	(1.38×1.38)R0°	12.08	11.5	0.44	0.07	3.0

potentials, while leaving the height of the plateaus unaltered. This general behavior is exemplified in Figure 3c, which shows σ_M versus E curves relative to different iodide concentrations. In Figure 4 this potential shift is plotted against log c, where c is the anionic concentration. More precisely, the potentials reported in Figure 4 correspond to two constant σ_M values, chosen along the rising section of the two consecutive σ_M versus E steps. The shift of the second, more positive step practically coincides with that of the peak potential of the sharp anodic peak in the corresponding cyclic voltammogram. The slopes of the plots in Figure 4 are just a measure of the Esin and Markov coefficient[17] $(\partial E/\partial \mu_i)_{\sigma M}$, where μ_i is the bulk chemical potential of the adsorbed anion. For the first, more negative σ_M versus E step, the slope of the E versus log c plot at constant σ_M equals −32 mV for sulfide, −74 mV for iodide, −64 mV for bromide, and −85 mV for chloride; for the second, more positive step, it equals −41 mV for sulfide, −59 mV for iodide, −70 mV for bromide and −72 mV for chloride.

The σ_M versus E curves for different concentrations of bromide, iodide, and sulfide ions, in the presence of a strong excess of supporting electrolyte, were integrated over potential, starting from a potential negative enough to exclude anionic chemisorption. In the case of chloride ion, the same procedure was applied to σ_M versus E curves relative to mixed solutions of cM KCl + (0.1 − c) M KPF_6. In view of the electrocapillary equation

$$-\mathrm{d}\gamma = \sigma_M\,\mathrm{d}E + RT\Gamma_i\,\mathrm{d}\ln c \qquad (2)$$

the resulting curves measure the interfacial tension γ, apart from an additive constant. As an example, Figure 5 shows curves of $[\gamma - \gamma(-1.3\ \mathrm{V})]$ versus E for different concentrations of bromide ion and for the supporting electrolyte alone. At these high bromide concentrations and over the whole potential range of stability of the $(\sqrt{3}\times\sqrt{3})$R30° structure, the plot of $[\gamma-\gamma(-1.3\mathrm{V})]$ versus ln c at constant E is linear, as shown in the inset of Figure 5; moreover, the slope, $(\partial\gamma/\partial \ln c)_E$ of this plot is independent of potential and measures $-RT\Gamma_i$ in view of eq 2. For bromide, iodide, and sulfide ions, the thermodynamic analysis of σ_M versus E curves was confined to the first plateau and hence to the $(\sqrt{3}\times\sqrt{3})$R30° overlayer. For chloride ions, the analysis was extended to the second plateau, corresponding to the (1.38×1.38)R0° structure. Table 1 summarizes Γ_i values obtained by the above thermodynamic procedure, to be compared with the

(17) Grahame, D. C. *Annu. Rev. Phys. Chem.* **1955**, *6*, 337.

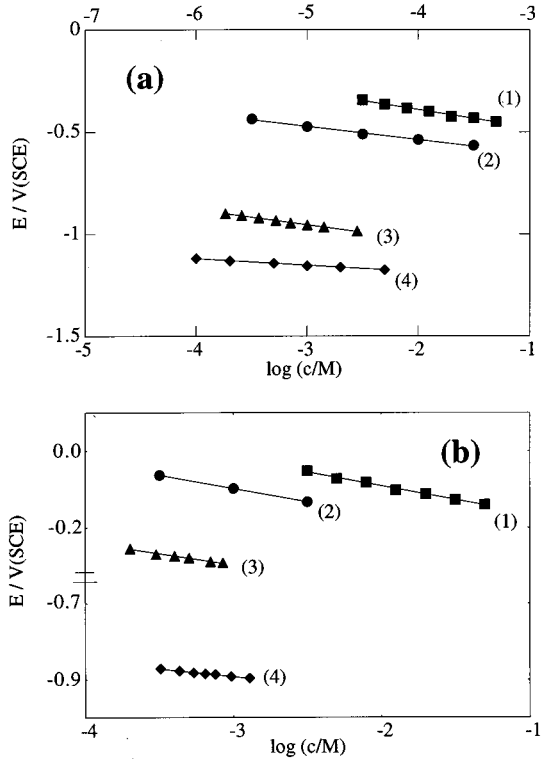

Figure 4. (a) Plots of E versus log c on Ag(111) from solutions of c M KCl + (0.1 − c) M KPF_6 at $\sigma_M = +53\ \mu C\ cm^{-2}$ (1), bromide in 0.1 M KPF_6 at $\sigma_M = +57\ \mu C\ cm^{-2}$ (2), iodide in 0.15 M NaOH at $\sigma_M = +12\ \mu C\ cm^{-2}$ (3), and sulfide in 0.15 M NaOH at $\sigma_M = +59\ \mu C\ cm^{-2}$ (4); the lower log c axis refers to plots 1, 2, and 4, and the upper one to plot 3. (b) E versus log c plots from the same solutions as in part a, for $\sigma_M = +80\ \mu C\ cm^{-2}$ (1), $\sigma_M = +98\ \mu C\ cm^{-2}$ (2), $\sigma_M = +78.8\ \mu C\ cm^{-2}$ (3), and $\sigma_M = +128\ \mu C\ cm^{-2}$ (4).

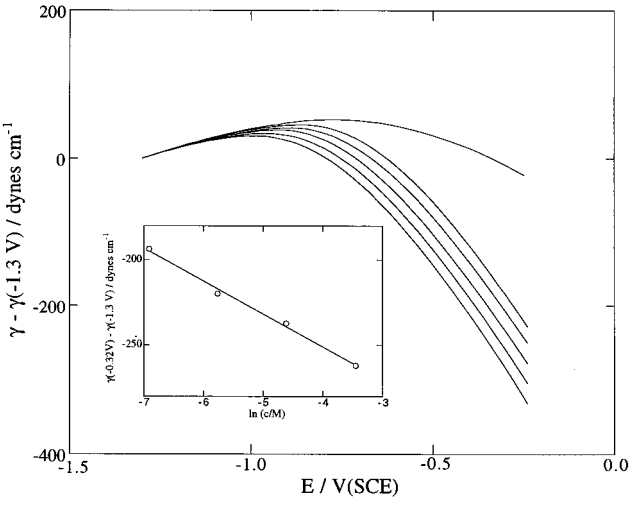

Figure 5. Plots of $[\gamma(E) - \gamma(-1.3\ V)]$ versus E on Ag(111) from bromide solutions in 0.1 M KPF_6. Proceeding downward, the bromide concentrations are 0, 3.16×10^{-4}, 1.0×10^{-3}, 3.16×10^{-3}, 1.0×10^{-2}, and 3.16×10^{-2} M. The inset is a plot of $[\gamma(E) - \gamma(-1.3\ V)]$ versus ln c at $E = -0.320$ V for the same experimental conditions.

corresponding "structural" values deduced from STM images. Except for the case of chloride ion, thermodynamic Γ_i values exceed the structural ones by about 5−10%; this can be explained by a moderate roughness of the Ag(111) face. Agreement between the two sets of Γ_i values can therefore be regarded as satisfactory.

The above experimental data allow us to estimate an "integral" value of the electrosorption valency, defined by

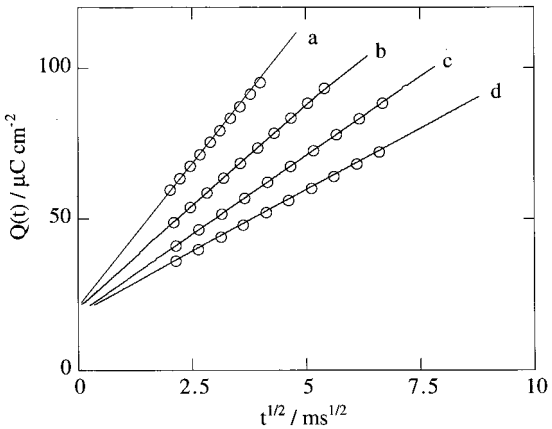

Figure 6. Plots of $Q(t)$ versus $t^{1/2}$ on Ag(111) from sulfide solutions of concentration 8.45×10^{-4} (a), 6.30×10^{-4} (b), 4.90×10^{-4} (c), and 3.80×10^{-4} M (d) in 0.15 M NaOH, as obtained by jumping from −1.40 to −0.90 V.

the equation

$$l_{B,int} \equiv -z(\sigma_M - \sigma_M^\circ)\sigma_i \qquad (3)$$

Here $(\sigma_M - \sigma_M^\circ)$ is the vertical distance between the σ_M versus E curves and the corresponding σ_M° versus E curves in Figure 3, measured over the potential range of stability of an ordered overlayer of surface concentration $\Gamma_i = \sigma_i/(zF)$. Over such a potential range $(\sigma_M - \sigma_M^\circ)$ is almost constant, since the two charge versus potential curves run practically parallel. Values of the $l_{B,int}/z$ ratio for the different anions and overlayer structures are summarized in Table 1. They were calculated by using the structural Γ_i values.

In the case of strongly chemisorbed species, such as halide and sulfide ions, an alternative chronocoulometric procedure can be used to estimate the electrosorption valency as a function of the applied potential. It consists of adopting bulk anionic concentrations c in the range from 10^{-4} to 10^{-3} M and of jumping from a fixed initial potential E_i, negative enough to exclude anionic adsorption, to a final potential E, where the anion is strongly adsorbed. Under these conditions, the charge density $Q(t)$ following the potential jump varies linearly with $t^{1/2}$ during the first 30−40 ms, even if this short period is followed by a process of polynucleation and growth yielding an ordered overlayer. Figure 6 exemplifies this behavior for sulfide adsorption at different bulk concentrations. The slopes of the $Q(t)$ versus $t^{1/2}$ plots are proportional to the bulk concentration c, as shown in Figure 7 for sulfide, iodide, and bromide adsorption. The adsorption of the supporting anion, no matter if specific or nonspecific, takes place in a few milliseconds after the potential jump, because of its relatively high bulk concentration. Conversely, the adsorption of sulfide or halide ions takes place more slowly, because of their low bulk concentrations. The time dependence of the charge density $Q(t)$ is therefore determined by the slow adsorption of the latter anions. The fact that $Q(t)$ satisfies the integral form of the Cottrell equation indicates that, at least during the first 30−40 ms after the potential jump, the adsorption of halide and sulfide ions is diffusion-controlled under limiting conditions, that is with the volume concentration at the electrode surface much smaller than the corresponding bulk value. Under these conditions, the intercept of the $Q(t)$ versus $t^{1/2}$ plots on the charge axis yields the charge density Q_0 following the potential jump $E_i \rightarrow E$ in the absence of the chemisorbed anion. Moreover, the surface charge density

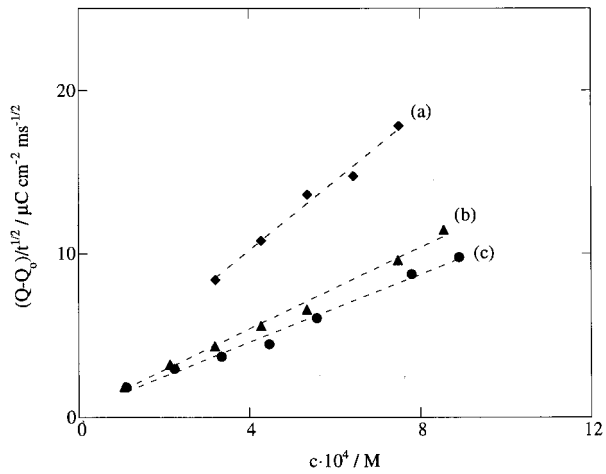

Figure 7. Plots of $(Q - Q_0)/t^{1/2}$ versus c on Ag(111) from solutions of sulfide in 0.15 M NaOH for a −1.40 V → −0.90 V jump (a), iodide in 0.15 M NaOH for a −1.50 V → −0.50 V jump (b), and bromide in 0.1 M KPF_6 for a −1.50 V → −0.35 V jump (c).

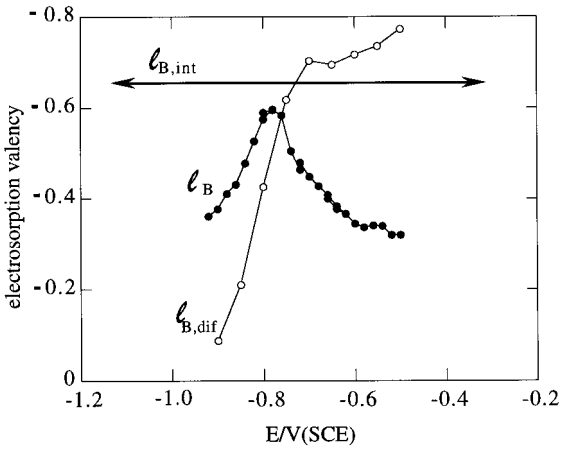

Figure 8. Plots of l_B (●) and $l_{B,dif}$ (○) against E for bromide adsorption on Ag(111). The horizontal arrow denotes the corresponding $l_{B,int}$ value. The quantities l_B, $l_{B,dif}$, and $l_{B,int}$ are defined in the text.

$\sigma_i(t)$ of the chemisorbed anion at a given time t, as expressed by the Cottrell equation, equals $2zF(Dt/\pi)^{1/2}c$, where D is its diffusion coefficient. Consequently, the electrosorption valency, again expressed by $-z[\sigma_M(t) - \sigma_M°]/\sigma_i(t)$, is simply proportional to the slope of the $Q(t)$ versus $t^{1/2}$ plot:

$$l_{B,diff} = -z\left[\frac{\sigma_M(t) - \sigma_M°}{\sigma_i(t)}\right] = -z\left[\frac{Q(t) - Q_0}{\sigma_i(t)}\right] = -\frac{\pi^{1/2}}{2FD^{1/2}c}\left[\frac{Q(t) - Q_0}{t^{1/2}}\right] \quad (4)$$

Values of the electrosorption valency $l_{B,dif}$ for bromide, iodide, and sulfide ions, obtained from the slope of the $Q(t)$ versus $t^{1/2}$ plots, are reported as a function of E in Figures 8−10. Values of the diffusion coefficients D were taken from the polarographic literature: 1.70×10^{-5} cm^2 s^{-1} for sulfide,[18] 1.72×10^{-5} cm^2 s^{-1} for iodide,[19] 1.86×10^{-5} cm^2 s^{-1} for bromide,[20] and 1.82×10^{-5} cm^2 s^{-1} for chloride.[21]

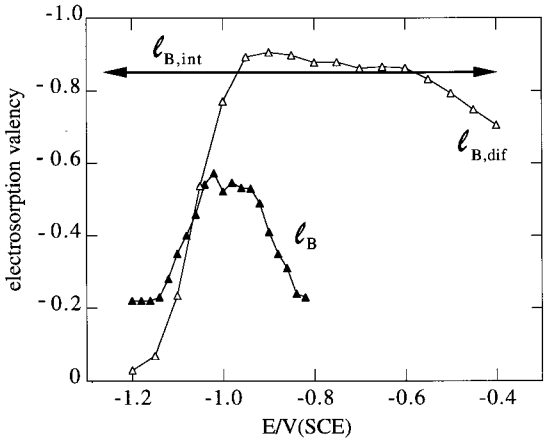

Figure 9. Plots of l_B (▲) and $l_{B,dif}$ (△) against E for iodide adsorption on Ag(111). The horizontal arrow denotes the corresponding $l_{B,int}$ value.

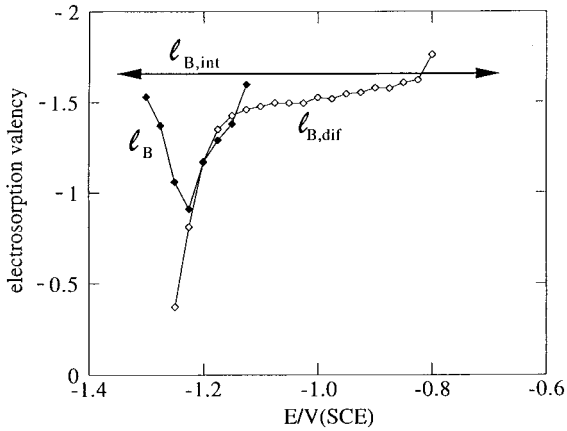

Figure 10. Plots of l_B (◆) and $l_{B,dif}$ (◇) against E for sulfide adsorption on Ag(111). The horizontal arrow denotes the corresponding $l_{B,int}$ value.

Figures 8−10 also report values of the electrosorption valency l_B obtained by the usual thermodynamic procedure, from the limiting slope of σ_M versus Γ_i plots at constant potential for $\Gamma_i \rightarrow 0$. The l_B values for sulfide were taken from ref 13, those for bromide were obtained from the adsorption data in ref 22, and those for iodide form part of chronocoulometric measurements of iodide adsorption on the low-index faces of Ag, to be published.[23] It is apparent that the l_B values differ appreciably from the corresponding $l_{B,dif}$ values. Both values increase rapidly over the potential range of the order−disorder two-dimensional phase transition, yielding the overlayer. However, when proceeding toward more positive potentials over the range of stability of the $(\sqrt{3}\times\sqrt{3})$R30° overlayer, $l_{B,dif}$ attains a roughly constant value that is close to the integral electrosorption valency $l_{B,int}$, while l_B for iodide and bromide decreases progressively. The decrease in l_B toward more positive potentials is to be ascribed to the inaccuracy in the estimate of the limiting slope of the σ_M versus Γ_i plots at constant potential for $\Gamma_i \rightarrow 0$. In fact, due to the gradual increase in adsorptivity of anions with an increase in potential, the latter increase causes the range of Γ_i values covered by the σ_M versus Γ_i plots to shift toward higher Γ_i values. This is shown in Figure 11, relative to iodide adsorption on Ag(111).[23] In

(18) Revenda, J. *Collect. Czech. Chem. Commun.* **1941**, *6*, 453.
(19) Beran, P.; Bruckenstein, S. *Anal. Chem.* **1968**, *40*, 1044.
(20) Peters, D. G.; Kinjo, A. *Anal. Chem.* **1969**, *41*, 1806.
(21) Gallego, J. M.; Castellano, C. E.; Calandra, A. J.; Arvia, A. J. *Electroanal. Chem.* **1975**, *66*, 207.
(22) Foresti, M. L.; Innocenti, M.; Kobayashi, H.; Pezzatini, G.; Guidelli, R. *J. Chem. Soc., Faraday Trans.* **1996**, *92*, 3747.
(23) Foresti, M. L.; Innocenti, M.; Kobayashi, H.; Guidelli, R. Unpublished results.

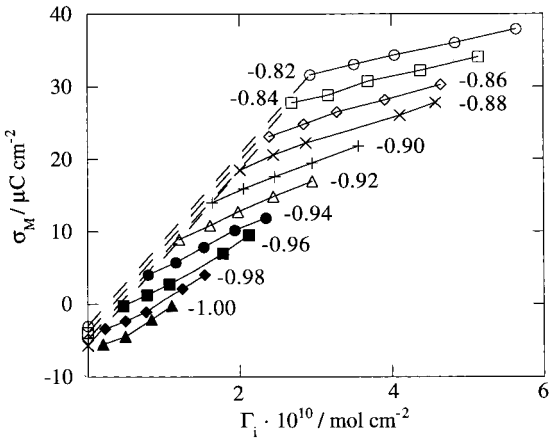

Figure 11. Plots of σ_M versus Γ_i at constant potential for iodide adsorption on Ag(111) from KPF_6 solutions. Numbers on each curve denote potential values in V/SCE.

view of the downward concavity exhibited by the σ_M versus Γ_i plots for halide adsorption, the limiting slope of the experimentally accessible segment of these plots decreases as this segment shifts toward higher Γ_i values. This is more evident if the experimental point corresponding to the lowest accessible Γ_i value at each potential is joined to the point on the $\Gamma_i = 0$ axis at the same potential, that is, the point obtained from the σ_M° versus E curve of the supporting electrolyte in the absence of the halide ion (see the dashed segments in Figure 11). The electrosorption valency $l_{B,dif}$ obtained from diffusion-controlled adsorption relies on measurements corresponding to the same small, initial amount of adsorbed material at all potentials and hence does not suffer from the above limitation. A similar, but slighter, decrease in the absolute value of the electrosorption valency l_B toward more positive potentials was reported by Lipkowski et al. for chloride[24] and bromide[25] adsorption on Au(111). In this case the slope of the σ_M versus Γ_i plots for the obtainment of l_B was estimated by also including the points on the $\Gamma_i = 0$ axis.

The difference between the $l_{B,diff}$ and l_B values in Figures 8−10 is to be ascribed to the appreciable change in the activity coefficient of the adsorbed species with varying E that is to be expected over the potential range corresponding to the onset of a two-dimensional phase transition. Thus, adsorption isotherms can be expressed under the general form $a \exp(-\Delta G_{ads}°/RT) = f(\Gamma_i)$, where a is the activity of the adsorbing species in the bulk solution, $\Delta G_{ads}°$ is the standard Gibbs energy of adsorption, and $f(\Gamma_i)$ is some function of Γ_i that measures the activity of the adsorbed molecules.[26] Therefore, from the definition of the electrosorption valency,[2a,b] it follows that

$$l_B = \frac{1}{F}\left(\frac{\partial \mu}{\partial E}\right)_{\Gamma_i} = \frac{RT}{F}\left(\frac{\partial \ln a}{\partial E}\right)_{\Gamma_i} = \frac{1}{F}\frac{d\Delta G_{ads}°}{dE} + \frac{RT}{F}\left(\frac{\partial \ln f(\Gamma_i)}{\partial E}\right)_{\Gamma_i} \quad (5)$$

where μ is the chemical potential of the adsorbing species. During the initial diffusion-controlled random adsorption, $f(\Gamma_i)$ practically coincides with Γ_i, and consequently the second term in the last member of eq 5 vanishes. However, at higher Γ_i values, the progressive clustering of the adsorbed molecules that accompanies the onset of two-dimensional condensation, following a positive shift in potential, is expected to decrease the activity coefficient of the adsorbate at constant Γ_i, and hence $f(\Gamma_i)$. This causes a decrease in l_B in view of eq 5.

Discussion

Estimating λ from values of the electrosorption valency requires a number of modelistic assumptions. However, it is reasonable to assume that the trend shown by the $l_{B,int}$ values in Table 1 (or the $l_{B,dif}$ values in Figures 8−10) for the series of similar anions herein examined reflects an analogous trend in the corresponding λ values. The order of decrease of the $l_{B,int}/z$ values in Table 1 (i.e., sulfide ≈ iodide > bromide > chloride) parallels the order of increase of Pauling's electronegativity, also reported in Table 1. This correlation, already pointed out by Schultze and Koppitz,[2c] simply indicates that the tendency of a chemisorbed anion to transfer its negative charge to a given metal substrate decreases with an increase in its electronegativity.

Table 1 also shows that the $l_{B,int}/z$ value for sulfide and bromide ions increases in passing from the $(\sqrt{3}\times\sqrt{3})$R30° structure to the more compressed structure that is formed at more positive potentials. An opposite trend is shown by iodide adsorption, whose $l_{B,int}/z$ value decreases in passing from the $(\sqrt{3}\times\sqrt{3})$R30° structure to the more compressed (8×8)R0° structure. The small amount of charge that accompanies this passage is apparent by comparing the size of the positive voltammetric peak for iodide in Figure 2 with those of the other anions. This apparently anomalous behavior can be explained by considering that the (8×8)R0° structure is a corrugated structure, where the average distance of the adsorbed iodide ions from the adjacent silver surface atoms is necessarily greater than that in the $(\sqrt{3}\times\sqrt{3})$R30° structure. This causes a decrease in the mixing of the iodide orbitals with the electronic states of the metal, and hence in partial charge transfer.

Some Modelistic Considerations. Let us denote by $x = \beta$ the distance of the center of charge of the chemisorbed anions from the electrode surface and by $x = d$ the thickness of the inner layer. If the adsorbed anion transfers a fraction λe of its charge to the metal, the potential difference $\Delta\phi$ across the inner layer is approximately expressed by the equation

$$\Delta\phi = \chi_{el} - \frac{4\pi N_w \langle\mu\rangle}{\epsilon_\infty} + \frac{4\pi d(\sigma_M - \lambda\sigma_i/z)}{\epsilon_\infty} + \frac{4\pi(d-\beta)(1+\lambda/z)\sigma_i}{\epsilon_\infty} \quad (6)$$

Here χ_{el} is the surface dipole potential due to electron spillover, N_w is the number of water molecules adsorbed per unit surface, $\langle\mu\rangle$ is the average value of the dipole-moment normal component of the adsorbed water molecules, and ϵ_∞ is a dielectic constant that accounts for the distortional polarization of the solvent molecules. The third term in eq 6 is the potential difference across the inner layer due to the charge density $(\sigma_M - \lambda\sigma_i/z)$ on the metal surface. The fourth term is the potential difference across the $(\beta < x < d)$ layer due to the residual charge density $(1 + \lambda/z)\sigma_i$ of the adsorbed ions at $x = \beta$. In the presence of a high electrolyte concentration, the potential difference across the diffuse layer can be neglected, and the constancy of $\Delta\phi$ implies that of the applied potential E. Within the limits in which the two dipole terms in eq

(24) Shi, Z.; Lipkowski, J. *J. Electroanal. Chem.* **1996**, *403*, 225.
(25) Shi, Z.; Lipkowski, J.; Mirwald, S.; Pettinger, B. *J. Chem. Soc., Faraday Trans.* **1996**, *92*, 3737.
(26) Delahay, P. *Double Layer and Electrode Kinetics*; Interscience: New York, 1965; p 81.

6 can be disregarded with respect to the two charge terms (usually a reasonable assumption), differentiation of σ_M with respect to σ_i at constant E in eq 6 yields the following expression for the electrosorption valancy:

$$l_B = -z\left(\frac{\partial\sigma_M}{\partial\sigma_i}\right) \approx -\lambda + \frac{d-\beta}{d}(z+\lambda) \qquad (7)$$

This expression is entirely analogous to that derived by Schultze and Koppitz,[2c] the only difference being represented by the fact that these authors use the "geometric factor" $g \equiv (\phi^{\beta-d}/\Delta\phi)$ in place of the "thickness ratio" $(d-\beta)/d$, where $\phi^{\beta-d}$ is the average potential difference between the $x=\beta$ and $x=d$ planes. As pointed out by Schultze and Vetter,[2b] the two quantities come to coincide only in case of a constant electric field within the inner layer. According to eq 7, in the case of total charge transfer ($\lambda=-z$), l_B becomes equal to z. At a metal surface covered by a compact overlayer of chemisorbed anions with total charge transfer, the dipole term due to the interfacial water molecules is expected to be practically the same as that at the metal surface in the absence of anionic adsorption, at the same applied potential. In fact, in the latter case σ_i equals zero and the two charge terms in eq 6 are replaced by the single term $4\pi d\sigma_M^\circ/\epsilon_\infty$. From a comparison between this term and the single charge term $4\pi d(\sigma_M+\sigma_i)/\epsilon_\infty$, relative to anionic adsorption with total charge transfer, it follows that, at constant $\Delta\phi \approx E$ + constant, σ_M° is practically equal to $(\sigma_M+\sigma_i)$. In other words, the overall charge density on the metal side experienced by the interfacial water molecules at constant potential is practically the same both in the absence of adsorption and in the presence of a compact adsorbed overlayer with total charge transfer. The average orientation of the interfacial water molecules is therefore practically the same. Differently stated, the inhomogeneous electron gas extends over the whole compact adsorbed overlayer, and the interfacial water molecules are merely shifted to the solution side upon adsorption. As far as the dipole term is concerned, the situation is clearly more involved in the case of partial surface coverage and/or partial charge transfer ($\lambda < -z$).

The underpotential deposition (upd) of a metal M, from a solution of its ion M^z, on a different metal of higher electronegativity is often marked by a sharp voltammetric cathodic peak. In a few cases (e.g, Pb[27–29] and Tl[30] upd on Ag(hkl)) the quantity $-Q/(zF)$, where Q is the negative charge density under the peak, has been compared with the surface concentration Γ_i of the deposited metal. In these cases, good agreement between $\Gamma_i=\sigma_i/(zF)$ and $-Q/(zF)$ has been found. Note that Q is just equal to $(\sigma_M-\sigma_M^\circ)$ in eq 3. Hence, such an agreement implies that $l_{B,int}$ equals z, that is, that charge transfer is complete. This indicates that, at least in the case of a compact overlayer and of total charge transfer, the contribution from the two dipole terms in eq 6 is indeed negligible or else is almost the same at constant potential both in the presence and in the absence of the overlayer.

In applying eq 7, the use of the "geometric factor" g in place of the "thickness ratio" $(d-\beta)/d$, is definitely more appropriate.[2b] In practice, however, both g and $(d-\beta)/d$ require modelistic considerations for their estimate, and hence their values are only roughly approximate. On the basis of a number of experimental data, Schultze and coworkers set g approximately equal to 0.2 in aqueous solution,[2c–e,g] although a value of 0.4 was also employed.[2f] Taking into account that the first monolayer of water molecules is by far the most strongly polarized by the interfacial electric field, here d will be set equal to the diameter, 3 Å, of a water molecule, while β will be equated to the radius of the adsorbed anion. This procedure is expected to underestimate somewhat the thickness ratio $(d-\beta)/d$ and hence to overestimate the partial charge-transfer coefficient derived from eq 7. The λ values thus obtained are summarized in Table 1. Note that the uncertainty in the thickness ratio becomes less critical for the estimate of λ the more l_B approaches z. Hence, even though the uncertainty in the λ values may be appreciable for bromide and, even more so, for chloride, the gradual increase of λ in passing from chloride to iodide and sulfide reflects a physical reality. Electron transfer is almost complete for the $(\sqrt{7}\times\sqrt{7})$ structure of sulfide ions, while it decreases progressively in the order $I^- > Br^- > Cl^-$.

The slopes of the E versus log c plots at constant σ_M in Figure 4 are relatively close to (albeit somewhat greater than) the corresponding values of $2.3RT/zF$. In other words, the dependence of E upon log c can be roughly expressed by the pseudo-Nernstian relationship

$$E \cong \text{constant} + (2.3RT/zF)\log c \quad \text{at constant } \sigma_M \qquad (8)$$

This behavior is readily explained by considering that crossdifferentiation of the electrocapillary equation yields the following expression for the Esin–Markov coefficient:

$$\frac{1}{RT}\left(\frac{\partial E}{\partial \ln c}\right)_{\sigma_M} = -\left(\frac{\partial\Gamma_i}{\partial\sigma_M}\right)_c \rightarrow \left(\frac{\partial E}{\partial \log c}\right)_{\sigma_M} = -\frac{2.3RT}{zF}\left(\frac{\partial\sigma_i}{\partial\sigma_M}\right)_c \qquad (9)$$

Now, it is well-known that σ_i versus σ_M plots at constant c for adsorbing anions are roughly linear, with slopes slightly less than -1. The fact that σ_i tends to $-\sigma_M$ in dilute solutions of pure salts of a specifically adsorbed anion is well documented[31–33] and has also been explained by Schmickler et al.[34] by simple model calculations. σ_M is relatively close to $-\sigma_i$, for sufficiently high values of $|\sigma_i|$, even in the presence of a constant excess of another electrolyte.[24,25,35] In fact, in this case, the relatively high ionic strength depresses the diffuse-layer charge, causing the charge σ_i to be neutralized mainly by the charge density σ_M on the metal. The slope of σ_i versus σ_M plots at constant c is slightly less than -1 even in mixtures of a salt of a specifically adsorbed anion with a nonspecifically adsorbed supporting electrolyte at constant ionic strength.[32,36–39] In view of eq 9, the slope of plots of E versus log c at constant σ_M is therefore expected to be close to $(2.3RT/$

(27) Lorenz, W. J.; Schmidt, E.; Staikov, G.; Bort, H. *Faraday Symp. Chem. Soc.* **1977**, *12*, 14.
(28) Bort, H.; Jüttner, K.; Lorenz, W. J.; Schmidt, E. *J. Electroanal. Chem.* **1978**, *90*, 413.
(29) Jüttner, K.; Lorenz, W. J. *Z. Phys. Chem.* **1980**, *122*, 163.
(30) Siegenthaler, H.; Jüttner, K.; Schmidt, E.; Lorenz, W. J. *Electrochim. Acta* **1978**, *23*, 1009.
(31) Dutkiewicz, E.; Parsons, R. *J. Electroanal. Chem.* **1966**, *11*, 100.
(32) Payne, R. *Trans. Faraday Soc.* **1968**, *64*, 1638.
(33) Sears, A. R.; Anson, F. *J. Electroanal. Chem.* **1973**, *47*, 521.
(34) Schmickler, W.; Henderson, D.; Hurwitz, H. D. *Z. Phys. Chem.* **1988**, *160*, 191.
(35) Shi, Z.; Lipkowski, J.; Mirwald, S.; Pettinger, B. *J. Electroanal. Chem.* **1995**, *396*, 115.
(36) Lawrence, J.; Parsons, R.; Payne, R. *J. Electroanal. Chem.* **1968**, *16*, 193.
(37) D'Alkaine, C. V.; Gonzalez, E. R.; Parsons, R. *J. Electroanal. Chem.* **1971**, *32*, 57.
(38) Hills, G. J.; Reeves, R. M. *J. Electroanal. Chem.* **1973**, *42*, 355.
(39) Valette, G.; Hamelin, A.; Parsons, R. *Z. Phys. Chem.* **1978**, *113*, 71.

zF), independent of whether partial charge transfer takes place. Differently stated, the fulfillment of eq 8 is by no means a proof of Nernstian charge transfer, that is, of complete charge transfer upon adsorption.

Any attempt to estimate λ directly through a Nernst-type equation

$$E = \text{constant} - (2.3RT/\lambda F) \log c \qquad (10)$$

is expected to yield a λ value close to $-z$, even in the absence of partial charge transfer. The same is true if slow adsorption is assumed, and a Butler−Volmer-type equation with Langmuirian adsorption is applied:

$$j = \lambda F\left\{k_{ads}c(1-\vartheta)\exp\left[(1-\beta)\frac{\lambda FE}{RT}\right] - k_{des}\vartheta\exp\left(-\beta\frac{\lambda FE}{RT}\right)\right\} \qquad (11)$$

where j is the current density, ϑ is the surface coverage by the adsorbed anion, and k_{ads} and k_{des} are the rate constants for adsorption and desorption. This explains why the use of eq 10 led Schmidt and Stucki[40,41] to conclude that chloride and bromide adsorption on polycrystalline Ag in the presence of a constant excess of $NaClO_4$ is characterized by an electrosorption valency l_B equal to -1. Likewise, the use of eq 11 led Jovic et al.[42] to conclude that chloride adsorption on the low-index faces of Ag occurs with complete charge transfer ($\lambda = 1$). As a matter of fact, Schmidt and Stucki based their conclusions on the potential shift with varying log c at constant σ_i, rather than at constant σ_M. However, from the properties of partial derivatives it follows that

$$\left(\frac{\partial E}{\partial \log c}\right)_{\sigma_i} = \left(\frac{\partial E}{\partial \log c}\right)_{\sigma_M} - \left(\frac{\partial E}{\partial \sigma_i}\right)_c\left(\frac{\partial \sigma_i}{\partial \log c}\right)_{\sigma_M}$$

Since the partial derivative $(\partial E/\partial\sigma_i)_c$ for chloride adsorption on the low-index faces of Ag in the presence of an indifferent electrolyte is anomalously low,[39] the potential shift with varying log c is expected to be practically the same at constant σ_i and at constant σ_M. Consequently, the results by Schmidt and Stucki do not prove a complete charge transfer upon chloride adsorption on silver. This may explain why their l_B values deviate notably from the Schultze and Koppitz plot showing the correlation between l_B/z and the absolute value of the difference in electronegativities between metal substrate and adsorbate (Figure 2 in ref 2c), while the values in Table 1 are in fairly good agreement with this plot.

In conclusion, direct procedures for the estimate of the partial charge-transfer coefficient λ that avoid the intermediate estimate of the electrosorption valency must be carefully checked, since they may often lead to erroneous results.

Acknowledgment. The financial support of the Ministero dell'Universita' e della Ricerca Scientifica and of the Consiglio Nazionale delle Ricerche is gratefully acknowledged.

LA980692T

(40) Schmidt, V. E.; Stucki, S. *Ber. Bunsen-Ges. Phys. Chem*. **1973**, *77*, 913.
(41) Schmidt, V. E.; Stucki, S. *J. Electroanal. Chem*. **1973**, *43*, 425.
(42) Jovic, B. M.; Jovic, V. D.; Drazic, D. M. *J. Electroanal. Chem*. **1995**, *399*, 197.